Intercomparison between the observed and modeled 21 January 2010 low topped tornado producing thunderstorm in Huntsville, AL

Elise V. Schultz, Cody Kirkpatrick, Udaysankar S. Nair, Christopher J. Schultz, Kevin R. Knupp
Department of Atmospheric Science, UAHuntsville, Huntsville, AL

Walter A. Petersen
NASA Marshall Space Flight Center, Huntsville AL

Lawrence D. Carey
Earth System Science Center, UAHuntsville, Huntsville, AL

1) Introduction

Detailed studies of low topped supercell thunderstorms are far less frequent than their larger, taller supercell brethren; however, these thunderstorms are still capable of producing significant severe weather that can affect life and property. Kennedy et al. (1993) observed a mini supercell tornadic storm in Colorado that did not have a vertical extent larger than 7 km, but did have similar characteristics to Great Plains supercells. Knupp et al. (1998) used observations and models to document a small but intense supercell storm in North Alabama, and noted that the storm did not have much lightning associated with it, but did have cyclic behavior and a strong convective core. Moreover, their numerical simulations determined the reasoning for the lack of observed lightning activity was due to insufficient concentrations of precipitation-sized ice to support effective charge separation by the non-inductive charging mechanism in spite of updraft magnitudes of 15-20 m s^{-1} in the mixed phase region of the storm. Markowski and Straka (2000) noted rotating updrafts in a low-buoyancy, highly sheared environment. The vertical extent of the cloud tops were 8-11 km high, but only for a short period of time. These storms did have similar characteristics of supercell storms on radar (e.g., hook echoes, velocity couplets, weak echo regions), and one of the storms was able to produce a tornado.

On January 21, 2010, a unique opportunity presented itself as several low topped supercells produced multiple reports of large hail (up to 7 mm in diameter) and two tornadoes in the Tennessee Valley region. Most of the severe weather occurred in South Central Tennessee as large hail (up to 7 mm in diameter) and a tornado were observed with in a group of four low topped supercells. However, the storm that caught the most attention was a low topped supercell that developed in North Central Alabama about 2200 UTC and trekked eastward towards Huntsville AL, producing an EF-2 tornado during the evening rush hour.

Herein we present observations and two numerical model simulations of the January 21, 2010, Huntsville, AL tornado. The goals of the study are 1) to use the suite

*Corresponding Author: Christopher J. Schultz, Department of Atmospheric Science, UAHuntsville, 320 Sparkman Dr., Huntsville AL, 35805, email: schultz@nsstc.uah.edu

of weather observing platforms in the Huntsville area to determine the storm's microphysical and electrical characteristics (Figure 1), 2) compare observations to three modeling simulations to better understand the formation and evolution of the thunderstorm, and 3) determine if topography played a role in the development of the tornado near Huntsville, AL.

2) Data and Model Setups

a. *Observational Platforms*

Several observational platforms collected valuable data on the thunderstorm that produced the Huntsville tornado. The most prominent is the Advanced Radar for Meteorological and Operational Research (ARMOR; Petersen et al. (2007)) 5 cm dual polarimetric radar located at the Huntsville International Airport. The radar is operational 24/7 with the ability for an operator to perform sectored volume scans on features of interest. A list of variables and radar characteristics is located in Table 1, along with the radar characteristics of the local WSR-88D radar at Hytop, AL (KHTX).

The ARMOR radar data following the event was processed to correct for attenuation. The reprocessed data were edited in the NCAR SOLOII program. Manual unfolding of aliased velocities and removal second trip and side lobe echoes was performed on these data. Next, the data were gridded to a Cartesian grid by the NCAR REORDER program and combined with KHTX data in CEDRIC to retrieve the three-dimensional wind field. However, since the supercell moved almost precisely along the baseline between ARMOR and KHTX, retrieval of dual Doppler winds for the tornadic portion of this thunderstorm was unavailable.

In addition to the radar instrumentation, total lightning information from the North Alabama Lightning Mapping Array (Koshak et al. 2004) was utilized to infer microphysical information.

Table 1 – Characteristics of the ARMOR and KHTX radars.

Radar Characteristics	ARMOR	KHTX
Beamwidth (deg)	1.1	1.0
Polarization	Linear, Simultaneous H and V (STSR)	Linear, H
Variables Collected	Z, Vr, SW, ZDR, ϱhv, Φdp	Z, Vr, SW
Wavelength (cm)	5.32	10.0
Nyquist Velocity (m/s)	16.1	23.5-35.0

This system consists of 14 stations and samples in 80 μs intervals, recording accelerating charge associated with lightning. Individual radiation sources associated with lightning are grouped into flashes using a clustering algorithm developed by McCaul et al. (2005b) and a minimum threshold for sources in a flash is set at 10 sources (Wiens et al. 2005).

Also included in the analysis are data from number of surface observations located at UAHuntsville. These observations include temperature, dew point, wind, and Parsivel and two 2 dimensional video disdrometers to determine rainfall characteristics in the forward flank of the storm (Carey et al. 2010, this conference 15.5).

b. *Idealized model setup*

To further analyze this rare event, an idealized simulation was conducted using the Regional Atmospheric Modeling System (RAMS), version 3b, as described in McCaul et al. (2005). This configuration of RAMS was found to reproduce observed storms reasonably well, at least in the qualitative sense (Kirkpatrick et al. 2007). The horizontally homogeneous environment is initialized with a blend of the 00 UTC 22 January 2010 soundings at Birmingham, AL (KBMX) and Nashville, TN (KBNA), modified with surface observations from Huntsville, AL (KHSV) at the same time. The storm is initialized using an LCL-conserving thermal bubble magnitude of 2.5 K, and is simulated on a 75 km x 75 km x 24.5 km domain with 500 m horizontal resolution (and roughly 500 m in the vertical), for 2 h of simulated time. Single-moment ice microphysics are included. While the horizontal grid spacing is insufficient to resolve tornado circulations explicitly, it should be adequate to resolve the evolution of the low level mesocyclone. Given that this model setup has no topography or surface or radiative fluxes, the purpose of this simulation is to evaluate the contribution of only the environmental profile to storm morphology, *in the absence of any terrain features.*

c. *RAMS nested grid model*

A nested grid configuration of three grids was used to establish a grid of 74 km x 74 km centered over Huntsville, AL with a grid spacing of 1 km. This grid was nested within a grid of 222 km x 222 km domain and 3km grid spacing, which in turn was located within a coarser outer grid of 12 km spacing and occupying a domain of 1200 km x 1200 km, both of which were also centered over Huntsville. A stretched vertical grid is utilized, with the grid spacing increasing by a factor of 1.1 from 40m at the surface to a constant value of 1km above the boundary layer. Analysis and forecast fields of atmospheric dynamic and thermodynamic fields from the North American Model is used to initialize all the three grids and to specify the temporally varying lateral boundary conditions on the outer grid. The modified Kuo convective parameterization scheme was utilized on outer coarse grid, while explicit cloud microphysical parameterization was activated on all the grids. A two-stream radiative transfer scheme that accounts for cloud radiative interactions was utilized. Surface topography, land use and vegetation characteristics were based on 1 km resolution USGS topography dataset, 30-second resolution Olson land use categorization data set and 1 km resolution Normalized difference vegetation index data respectively. Soil texture was specified using global 1 degree United Nations Food and Agricultural Organization data.

3) Observations and Results

a. *Observations*

This storm developed in Lawrence Co, AL about 2200 UTC. During this period, the radar operator was focused on several severe weather producing low topped storms in South Central Tennessee, therefore only radar observations from the lowest tilts were available prior to 2300 UTC. Around 2305 UTC, the forward flank downdraft passed over the UAHuntsville observing station at the National Space Science and Technology Center (NSSTC), where extremely large drops were observed by the disdrometer instrumentation. Average drop sizes were between 3-4 mm and the largest drops were on the order of 5-6 mm in diameter. The total flash rate of the thunderstorm was very small (maximum of 1 flash min^{-1}), and the maximum vertical extent of the storm was about 8 km.

At 2310 UTC an appendage developed on the rear flank of the storm (Figure 2) along with a fine line just to the south of the appendage. . A long thin rear flank downdraft is present at this time, and this is due to the 20 knots of speed shear in the lowest 1 km of the environment.

Two minutes later at 2312 UTC, the appendage developed a hook feature, and the fine line became better defined. Also, one of the hills northeast of Redstone Arsenal "lights up" in the image (Figure 3, white circle) which is due to a change in pressure, temperature or humidity, and is indicative of a boundary. As time passed, the RFD/boundary feature remained present. The large differential reflectivity (ZDR) values indicated horizontally oblate particles, indicative of large hydrometeors (big drops and melting hail), and confirmed using disdrometer data collected at the NSSTC.

The next image at 2318 UTC (Figure 4) is one minute after the tornado had touched down on the lee side of the hills northeast of Redstone Arsenal. A hook echo was still clearly inside of the appendage, along with a ball of reflectivity just to the south of the hook echo. Figure 5 showed the storm three minutes later as the tornado is moving across I-565 just west of downtown Huntsville. A well defined hook was now present, along with an apparent debris ball (ρhv below 0.70 collocated with reflectivity greater than 25 dBZ). A 55 dBZ core extended up to 5 km, but the maximum height of the storm was near 9 km as a small overshoot of 25 dBZ extended to this level.

At 2323 UTC the circulation was identifiable at the surface despite the lack of a condensation funnel all the way to the surface. Several power poles were snapped and lighter debris (e.g., leaves, grass) were visible in the air. The most intriguing characteristic is that because the dew points were in the low to mid 50s across the area, the funnel was easily observable throughout its lifetime.

At 2328 UTC the storm reached the Five Points region of Huntsville and produces its highest rated damage. The vertical locations of VHF source points associated with lightning flashes are confined to the lowest 5 km of the storm, and the total flash rate for the storm was maximized at 2332 UTC (4 flashes min^{-1}) as the tornado ascends Monte Sano mountain. The tornado dissipated at 2334 UTC and this storm did not produce any additional severe weather during the rest of its lifetime.

b. *Idealized Model Observations*

The idealized storm remained "low-topped," with no appreciable updraft above about 8-9 km AGL. The shallow nature of the updraft, a small surface precipitation footprint (about 10 km across in the E-W direction), and evidence of a reflectivity appendage on the storm's southwestern flank (with strong vorticity on the eastern edge of this appendage, likely related to the rear-flank downdraft) give this storm the appearance of a mini-supercell (Figure 6). The strong low-level vorticity was acquired by the storm during the simulation's second hour, after the influence of the initiating disturbance had diminished. This strong rotation persisted even as the storm top began to decrease to about 6 km AGL in the last 15 min of the simulation. Maximum vorticity values at the lowest model level (126 km AGL) approached 0.02 s^{-1}, which would be among the largest values produced by low-CAPE storms in the robust simulation archive of Kirkpatrick et al. (2006).

c. *RAMS Nested Grid Model Output*

Two numerical modeling experiments were conducted with nested grids, the control (CTL) and the homogeneous terrain experiment (AVGTOPO). In the AVGTOPO experiment, the topography within the inner two grids is replaced by the domain averaged topography value. Both the simulations are integrated for a period of 12 hours starting from 1200 UTC. A convective storm with maximum cloud tops of about 8 km developed in the in 1 km grid between 2300-0000 UTC, the time period of interest for this study. Whereas the structure of storm in the CTL simulation was consistent with the radar observations, the time of formation and location of the simulated storm differed in comparison to observations. The simulated storm formed approximately 20 km northeast of Huntsville and an elongated feature was found extending to the southeast, similar to the pattern found in the radar reflectivity field (Figure 7). However, the AVGTOPO experiment, failed to develop convective clouds within the inner grid. Since the idealized, horizontally homogenous simulations forced by a thermal bubble and the CTL simulation both developed convection with features similar to observations, it appears that the role of the topography is to provide a triggering mechanism for convective cloud formation. Initial numerical model simulations thus suggest that topography did not have an influence on the morphology or intensification of the convective system.

4) Discussion and Conclusions

The presence of low topped supercells is fairly common (e.g., Schultz. et al. 2010, this conference), and thus understanding the characteristics of these storms is very important to protecting life and property in the future. These storm types contain similar characteristics to that of their larger Great Plains counterparts as observed in this study, but are not as large.

The most interesting observations of this low topped storm were:

1. Vertical extent was maximized at 9 km.
2. Large raindrops (5-6 mm) and melting hail in the storm’s forward flank downdraft.
3. Presence of a boundary and its subsequent interaction with the rear flank downdraft and hook echo.
4. The long thin rear flank downdraft due to the 20+ knots of speed shear in the lowest 1 km.
5. Lack of total lightning due to limited charge microphysics and

6. lack of vertical extent of the charging layers.
6. Development of the tornado on the lee side of the hills just to the northeast of Redstone Arsenal and demise of the tornado near Monte Sano mountain.

These observations match up quite nicely with the RAMS idealized model study. The storm within the model was limited in height to 8 km, however, contained a strong reflectivity core, and exemplified strong rotation within its right flank. This simulation demonstrates that it *is in fact possible* for a storm in this environment to produce strong low level rotation *even without the enhancing effects of surface topography.* This does not mean, however, that existing terrain features cannot serve to augment (or weaken) a storm's low level mesocyclone, through direct interaction or through enhancement of environmental storm-relative helicity via channel flows, for example (Schneider, 2009).

The RAMS nested grid output developed a storm that resembled the tornadic low topped supercell, but did not have the location and initial development time correct. The reflectivity structure that developed in this simulation was similar to that of the radar observations, with a strong convective core, and appendage off of the rear flank of the system. The height of this simulated storm was 8 km deep between 2300-0000 UTC, and topography had some influence on the development of these storms. However, these two simulations also suggest that topography may not have had much influence on the intensification of the system. Simulations will continue to be performed to try to accurately match up the simulated storm with the observations from radar. Additional analysis of why, in the absence of topography, only one of two idealized simulations produced sustained convection must also be performed.

Further analysis will need to be performed on this case to determine why the least threatening thunderstorm within this group of severe storms that developed on January 21, 2010 produced the most damaging tornado. Understanding this case will help forecasters anticipate these lower end tornado events that are commonly observed, thus increasing forecaster confidence and helping to disseminate warnings in a more efficient manner to the public.

5) References

Carey, L. D. W. A. Petersen, M. Thurai, M. E. Anderson, E. V. Schultz, C. J. Schultz, and K. Knupp, 2010: Precipitation properties of a cool-season tornadic storm inferred from C-band dual-polarimetric radar and 2D-video disdrometer observations. *25th Conf. on Severe Local Storms*, Denver, CO, Amer. Met. Soc.

Kennedy, Patrick C., Nancy E. Westcott, Robert W. Scott, 1993: Single-Doppler Radar Observations of a Mini-Supercell Tornadic Thunderstorm. *Mon. Wea. Rev.*, **121**, 1860–1870.

Kirkpatrick, C., E. W. McCaul, Jr., and C. Cohen, 2006: The effects of eight basic environmental parameters on the low-level rotation characteristics of simulated convective storms. *23rd Conference on Severe Local*

Storms, St. Louis, November 6-10, 2006, CD-ROM, 16.3.

Kirkpatrick, C., E. W. McCaul, Jr., and C. Cohen, 2007: The motion of simulated convective storms as a function of basic environmental parameters. *Mon. Wea. Rev.*, **135,** 3033-3051.

Knupp, K. R., J. A. Stalker and E. W. McCaul Jr, 1998: An observational and numerical study of a mini-supercell storm. *Atmos. Res.*, **49**, 35-63.

Koshak, W. J., and Coauthors, 2004: North Alabama Lightning Mapping Array (LMA): VHF Source Retrieval Algorithm and Error Analyses. *J. Atmos. Oceanic Technol.*, **21**, 543–558.

McCaul, E. W., Jr., C. Cohen, and C. Kirkpatrick, 2005: The sensitivity of simulated storm structure, intensity, and precipitation efficiency to environmental temperature. *Mon. Wea. Rev.*, **133,** 3015-3037.

McCaul, E. W., J. Bailey, J. Hall, S. J. Goodman, R. Blakeslee, and D. E. Buechler, 2005b: A flash clustering algorithm for North Alabama Lightning Mapping Array data. Preprints, Conf. on Meteorological Applications of LightningData, SanDiego, CA, Amer. Meteor. Soc., 5.2. [Available online at http://ams.confex. com/ams/Annual2005/techprogram/ paper_84373.htm.]

Markowski, Paul M., Jerry M. Straka, 2000: Some Observations of Rotating Updrafts in a Low-Buoyancy, Highly Sheared Environment. *Mon. Wea. Rev.*, **128**, 449–461.

Petersen, W. A., K. R. Knupp, D. J. Cecil, and J. R. Mecikalski, 2007: The University of Alabama Huntsville THOR Center instrumentation: Research and operational collaboration. INVITED PRESENTATION, 33rd International Conference on Radar Meteorology, American Meteorological Society, Cairns, Australia, August 6-10, 2007.

Schneider, D. G., 2009: The impact of terrain on three cases of tornadogenesis in the Great Tennessee Valley. *E. Journal of Operational Meteorology,* Nat. Wea. Assoc., 2009-EJ11.

Schultz, C. J., W. A. Petersen and L. D. Carey, 2010: Total lightning trend analysis of low-topped supercells across the Tennessee Valley. *25th Conf. on Severe Local Storms*, Denver, CO, Amer. Met. Soc.

Wiens, K. C., S. A. Rutledge, and S. A. Tessendorf, 2005: The 29 June 2000 supercell observed during steps. Part II: Lightning and charge structure. J. Atmos. Sci., 62, 4151–4177.

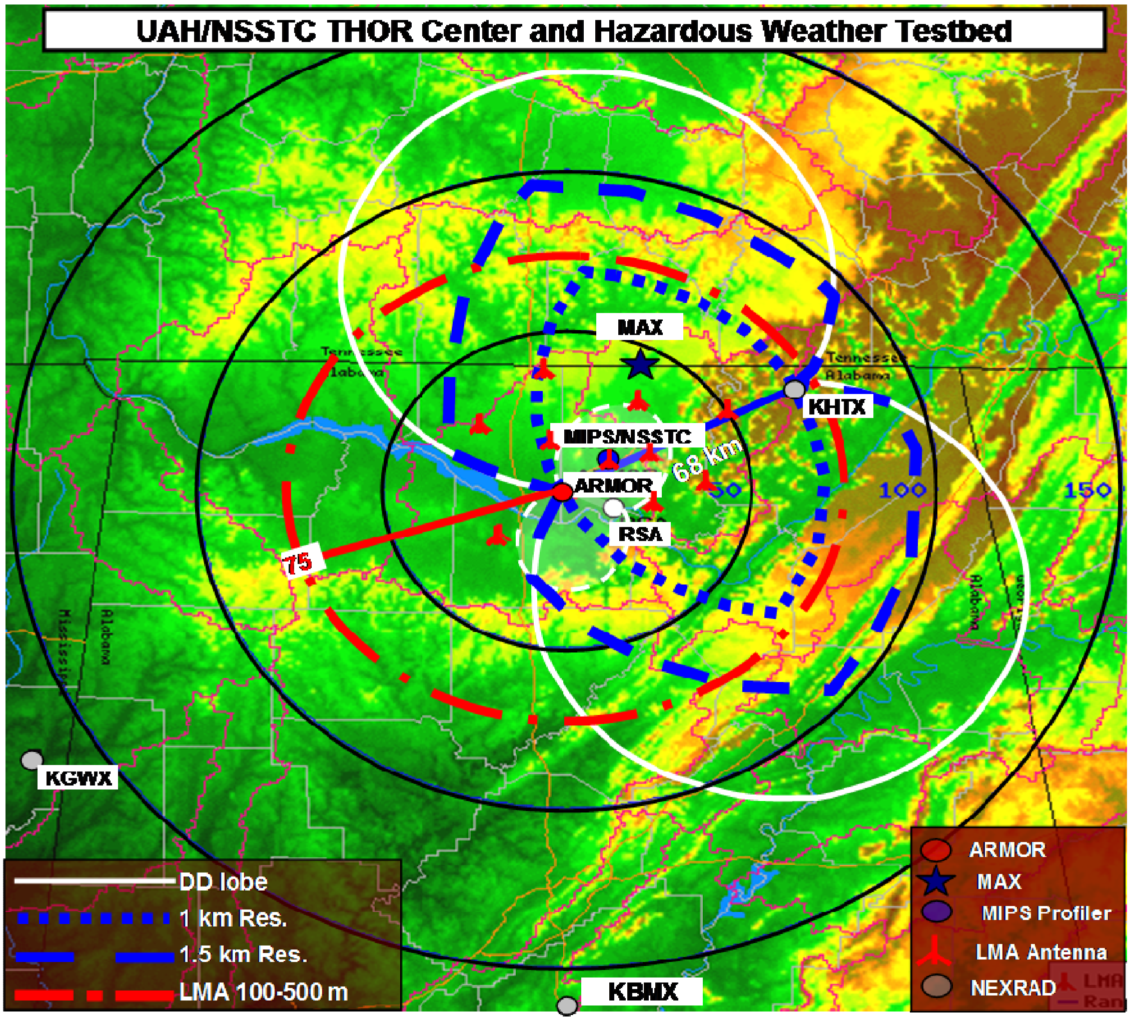

Figure 1 – An overview of the UAH/NSSTC THOR and Hazardous Weather Testbed (Petersen et al. 2007). Positions of ARMOR, the lightning mapping array antennae and other instrumentation that was unavailable on the day of the tornado (e.g., MAX, MIPS). All disdrometers are located at the NSSTC location.

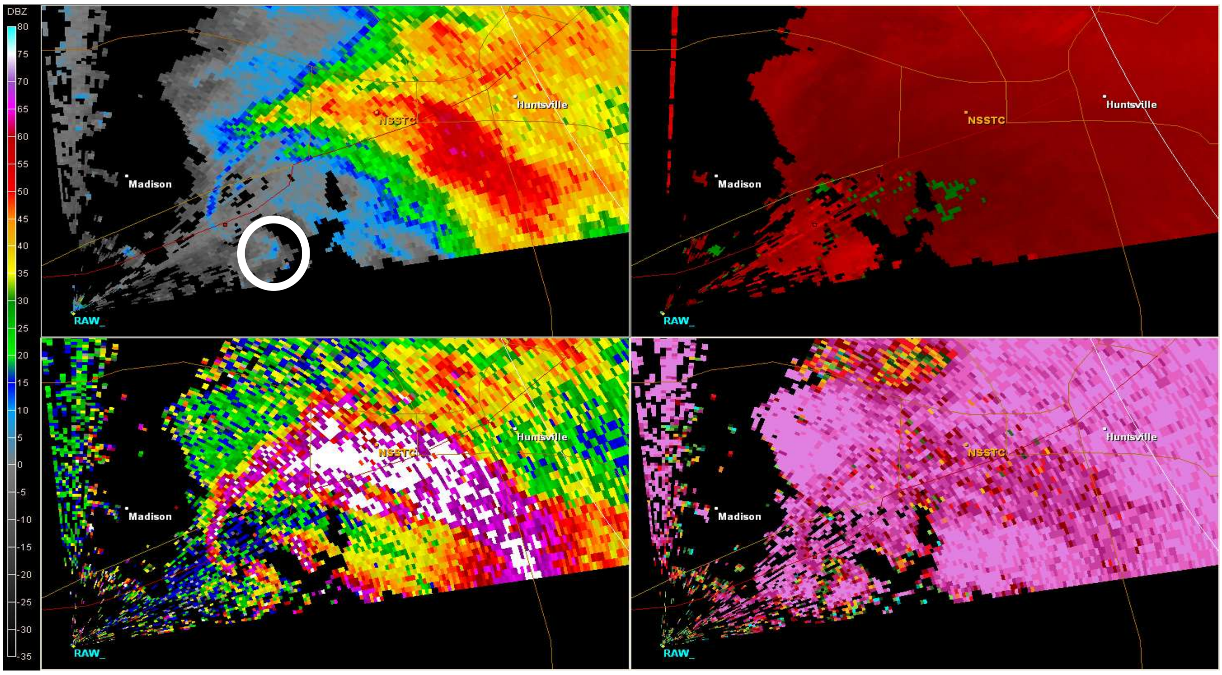

Figure 2 - Uncorrected ARMOR data at 2310.01 UTC at 2.0 degrees. Variables for each time are DZ, VR, ZDR, and ϱhv. The white circles in the DZ fields show where the refractive index changes causing the radar to "light up" one of the hills on Redstone Arsenal. This could be caused by a change in pressure, temperature or humidity which could be indicative of a boundary.

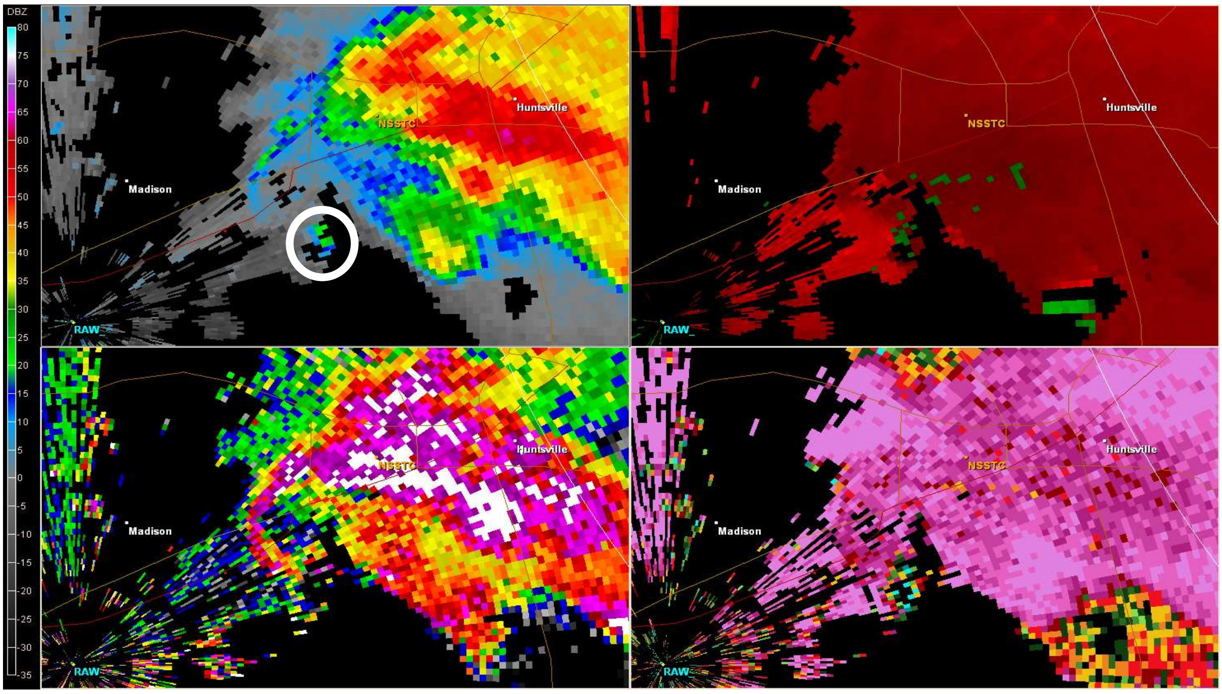

Figure 3 - Uncorrected ARMOR data at 2312.20 at 2.0 degrees. Variables for each time are DZ, VR, ZDR, and ϱhv. The white circles in the DZ fields show where the refractive index changes causing the radar to "light up" one of the hills on Redstone Arsenal. This could be caused by a change in pressure, temperature or humidity which could be indicative of a boundary.

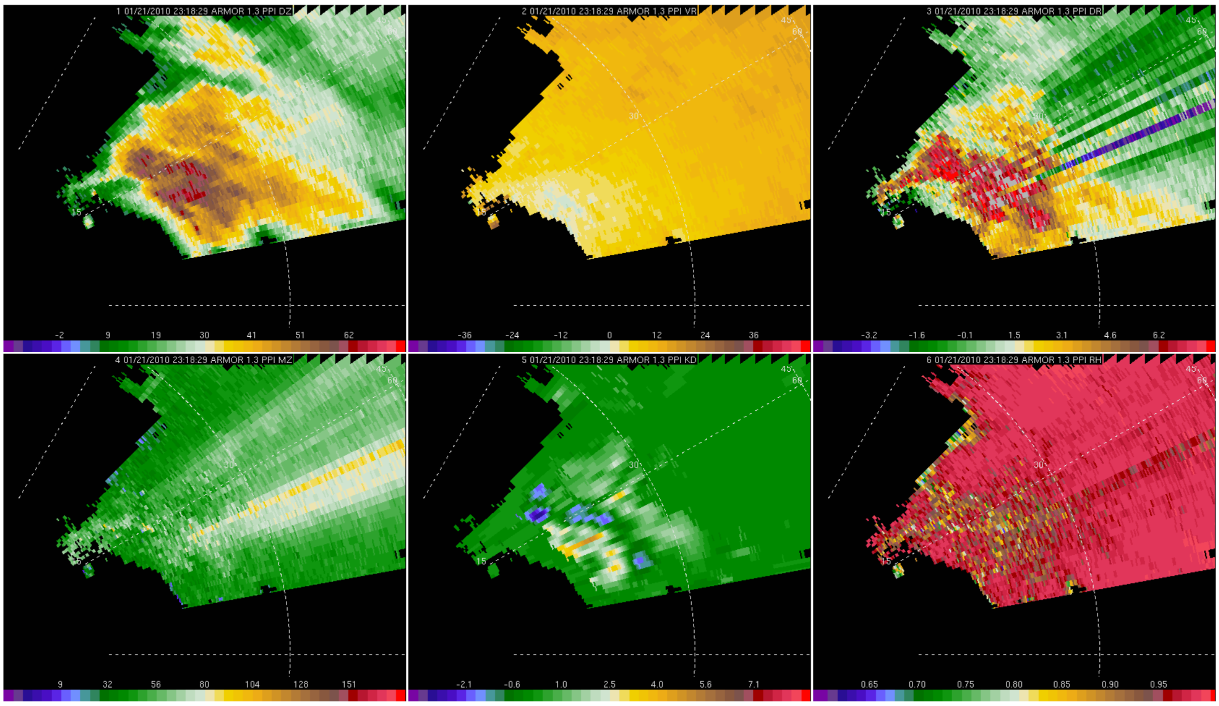

Figure 4 - Corrected ARMOR data at 2318.29 at 1.3 degrees. The tornado has already touched down on Redstone Arsenal a minute prior to this scan. A ball of reflectivity is located just ot the south of the hook echo.

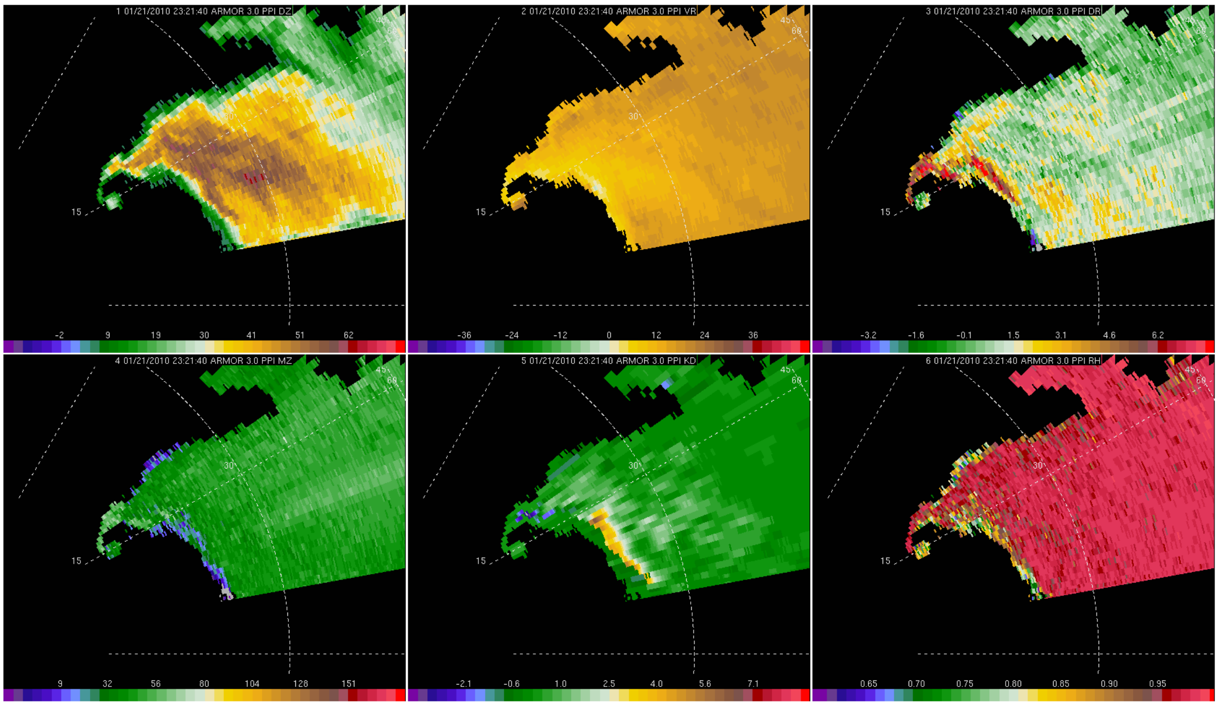

Figure 5 - Corrected ARMOR data at 2321.40 UTC at 3.0 degrees. A possible debris is visible in the hook region of the storm in RH in the lower right image.

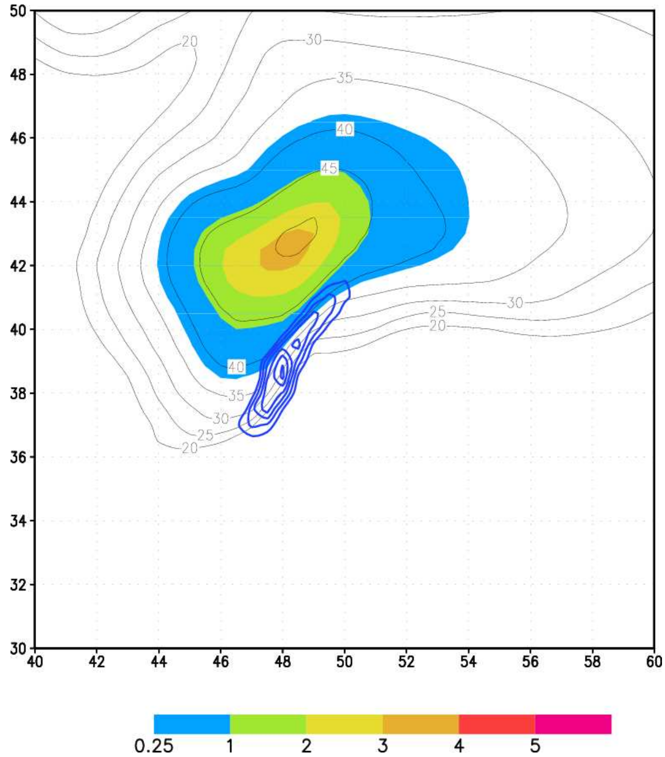

Figure 6 - Idealized simulation representing the 21 January tornadic storm. Shaded is surface rainwater mixing ratio (g kg^{-1}). Dark contours represent surface vorticity (in increments of 0.0025 s^{-1}, beginning at 0.005 s^{-1}), and light contours give the equivalent reflectivity factor in dBZ.

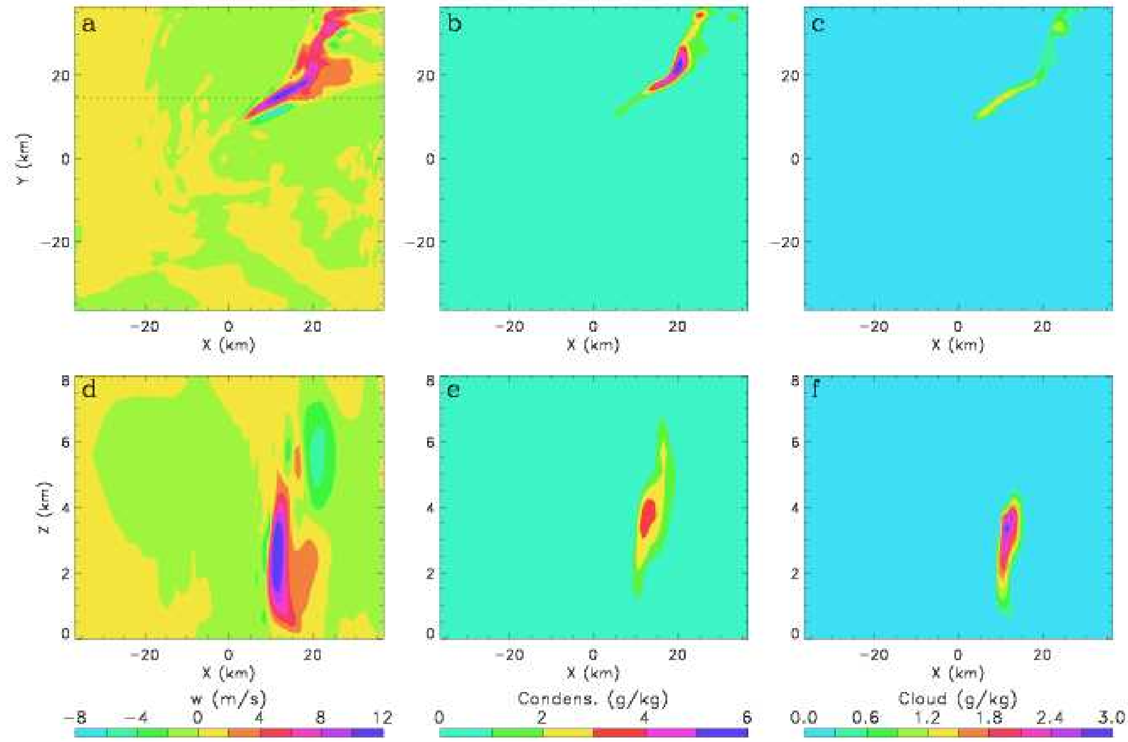

Figure 7 - Horizontal and vertical cross sections of the RAMS simulated vertical velocity, total condensate mixing ratio and cloud water mixing ratio are shown in panels a, b,c and d, e,f respectively. The cross section are for grid 4, valid at 2330 UTC on 21 January, 2010. The horizontal cross section is for height level of ~2 km, while the vertical cross section is along the dashed line shown in panel a.